

Super-Robust Nonadiabatic Holonomic Quantum Computation in coherence-protected Superconducting Circuits

Yuan-Sheng Wang,^{1,2} Zhaofeng Su,^{3,4,*} Xiaosong Chen,^{1,5,†} and Man-Hong Yung^{6,7,8,9,‡}

¹*School of Systems Science, Beijing Normal University, Beijing 100875, China*

²*School of Electronics and Information Engineering, Suzhou Vocational University, Suzhou 215104, China*

³*School of Computer Science and Technology, University of Science and Technology of China, Hefei 230094, China*

⁴*CAS Key Laboratory of Wireless-Optical Communications,*

University of Science and Technology of China, Hefei 230026, China

⁵*Institute for Advanced Study in Physics and School of Physics, Zhejiang University, Hangzhou 310058, China.*

⁶*Shenzhen Institute for Quantum Science and Engineering,*

Southern University of Science and Technology, Shenzhen, 518055, China.

⁷*International Quantum Academy, Shenzhen, 518048, China.*

⁸*Guangdong Provincial Key Laboratory of Quantum Science and Engineering,*

Southern University of Science and Technology, Shenzhen, 518055, China.

⁹*Shenzhen Key Laboratory of Quantum Science and Engineering,*

Southern University of Science and Technology, Shenzhen, 518055, China.

(Dated: October 11, 2024)

The scheme of nonadiabatic holonomic quantum computation (NHQC) offers an error-resistant method for implementing quantum gates, capable of mitigating certain errors. However, the conventional NHQC schemes often entail longer operations concerning standard gate operations, making them more vulnerable to the effects of quantum decoherence. In this research, we propose an implementation of the Super-Robust NHQC scheme within the Decoherence-Free Subspace (DFS). SR-NHQC has demonstrated robustness against Global Control Errors (GCEs). By utilizing capacitance-coupled transmon qubits within a DFS, our approach enables universal gate operations on a scalable two-dimensional square lattice of superconducting qubits. Numerical simulations demonstrate the practicality of SR-NHQC in DFS, showcasing its superiority in mitigating GCEs and decoherence effects compared to conventional NHQC schemes. Our work presents a promising strategy for advancing the reliability of quantum computation in real-world applications.

I. INTRODUCTION

Quantum computation is a new paradigm for solving computing tasks based on quantum mechanism [1]. Due the magic properties of entanglement and nonlocality in quantum mechanics [2–4], the corresponding quantum computation has the potential to efficiently solve certain hard problems that are intractable for classical computers, which is known as quantum advantages [5]. The advantage of quantum computation has been not only analyzed in theory but also demonstrated in experiments, such as the simulation of quantum systems [6, 7], factoring of prime numbers [8–10], searching unsorted data bases [11] and machine learning [12–14].

However, the current state of quantum computation is in the noisy intermediate-scale quantum (NISQ) era, characterized by the fact that the physical qubits are not enough for building fault-tolerant logical qubits to realize quantum advantage in practical difficult problems [15]. Thus, it is significant to design quantum gates with high-fidelity and robust control. Different error suppression protocols have been proposed to mitigate control errors in implementing quantum gates, which include dynamically corrected gates [16, 17], composite pulses [18, 19], geometric and holonomic quantum computation (GQC and HQC) [20]. Among these protocols,

HQC is a promising approach for universally designing robust quantum gates [21].

Quantum holonomies, including Abelian and non-Abelian ones, are global properties of quantum state spaces depending solely on the evolution paths of quantum systems, thereby also referring as the Abelian geometric phases and non-Abelian geometric phases, respectively [20]. Thus, the logical gates of HQC rely on quantum holonomies inherently possess resilience to a range of quantum errors [22–26]. HQC was firstly proposed for adiabatic holonomies [27] and has been designed for quantum computation based on a variety of physical systems [28–31]. However, the adiabatic processes are slow in time so that the corresponding applications are susceptible to decoherence and inducing considerable errors. On the contrary, the nonadiabatic approaches are faster and easier to realize than the adiabatic processes. Therefore, it is more practical to implement quantum gates with nonadiabatic evolutions. And HQC was subsequently generalized to scenarios utilizing nonadiabatic non-Abelian geometric phases [32–37]. The nonadiabatic HQC has been experimentally demonstrated in various systems, including superconducting circuits [38, 39], liquid NMR [40], cold atoms [41], trapped ions [42], nitrogen-vacancy centers in diamond [43–45], etc.

The author and their collaborators have proposed a new nonadiabatic holonomic quantum computation (NHQC) scheme referred as Super-Robust NHQC (SR-NHQC) in a recent research work [37]. This scheme provides the enhanced robustness against a specific kind of control error known as the global control error. The nonadiabatic property allows for

* zfsu@ustc.edu.cn

† chenxs@bnu.edu.cn

‡ yung@sustech.edu.cn

a shorter exposure time of qubits to undesired external influences. However, in most cases, the gate run time of this scenario is still longer than that of standard NHQC and trivial dynamical gates, indicating a higher sensitivity to decoherence.

In this paper, we propose a scheme for implementing the SR-NHQC within a decoherence-free subspace (DFS). This scheme is based on scalable coupling and layout configurations of transmon qubits. We conduct simulations using realistic decoherence parameters to evaluate the performance of various quantum computation protocols, including our proposed method, under the influence of decoherence. By comparing the performance across different schemes, we demonstrate the practicality and superiority of our approach, highlighting its potential for robust and reliable quantum computation.

This paper is organized as follows. In Sec. II, we develop universal single-logical-qubit gates in a DFS of three qubits for SR-NHQC. In Sec. III, we introduce a nontrivial two-logical-qubit SR-NHQC gate encoding in a two-excitation subspace of four qubits. We finally summarize the contribution and outlook of this research in Sec. IV.

II. UNIVERSAL SINGLE-LOGICAL QUBIT GATES

This section introduces the encoding of a single logical qubit within the DFS of three capacitively coupled transmons, and how to implement a universal single-logical-qubit gate. Additionally, we demonstrate how SR-NHQC in DFS effectively mitigates the global control errors (GCEs) in the presence of decoherence.

A. Tunable coupling through parametric modulations

For two capacitively coupled transmon qubits Q_{j_1} and Q_{j_2} , the Hamiltonian can be well approximated by [46, 47]

$$H = H_0 + H_{j_1 j_2}, \quad (1)$$

in this section, we only consider states in the subspace spanned by $\{|0_{j_1}\rangle, |1_{j_1}\rangle, |0_{j_2}\rangle, |1_{j_2}\rangle\}$, where $|0_{j_\alpha}\rangle$ ($|1_{j_\alpha}\rangle$) is the ground state (first excited state) of Q_{j_α} , in this subspace, the first term of RHS of Eq. (1) can be written as $H_0 = \sum_{m=j_1, j_2} \omega_m \sigma_z^{(m)}/2$ (for simplicity, we set $\hbar = 1$ here and after), and the second term reads $H_{j_1 j_2} = g_{j_1 j_2} (\sigma_{j_1}^+ + \sigma_{j_1}^-)(\sigma_{j_2}^+ + \sigma_{j_2}^-)$, with ω_j the transition frequency of Q_j , $g_{j_1 j_2} = g_{j_2 j_1}^*$ the static coupling strength, $\sigma_z^{(j)}$ the Pauli z operator of Q_j , $\sigma_j^- = |0\rangle_j \langle 1|$ and $\sigma_j^+ = |1\rangle_j \langle 0|$ the ladder operators with $\{|0\rangle_j, |1\rangle_j\}$ the computational basis of Q_j .

The Hamiltonian in the interaction picture reads $H_I(t) = U_0^\dagger(t) H_{j_1 j_2}(t) U_0(t)$, where $U_0(t) = \mathcal{T} \exp[-i \int_0^t H_0(t') dt']$. The transmon Q_{j_1} can be biased by an AC magnetic flux to periodically modulate its frequency as [47, 48]:

$$\omega_{j_1}(t) = \omega_{j_1} + \epsilon_{j_1} \sin(\nu_{j_1} t + \phi_{j_1}), \quad (2)$$

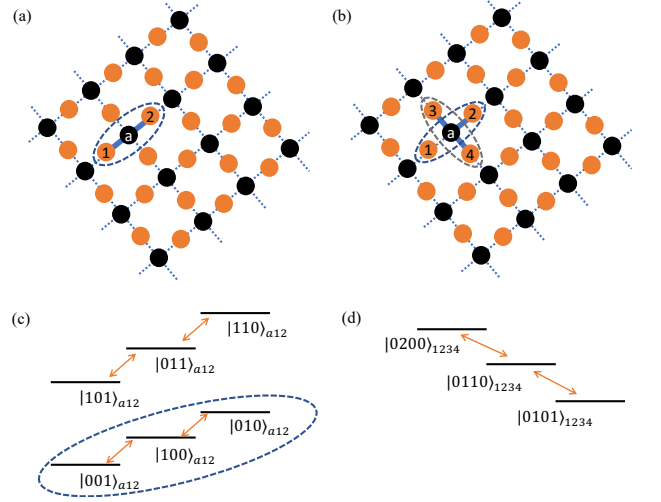


FIG. 1. The setup of our proposal: (a) A logical qubit or (b) two coupled logical qubits can be encoded in a scalable square array of coupled superconducting transmons. (c) Energy spectrum for three parametrically tunable coupled qubits, where the single-excitation subspace enables single-logical-qubit holonomic gates. (d) Energy spectrum for four parametrically tunable coupled qubits, where the two-excitation subspace enables the two-logical-qubit holonomic gate.

by using the Jacobi-Anger identity, $H_I(t)$ can be written in the following form

$$H_I(t) = \sum_{n=-\infty}^{\infty} i^n g_{j_1 j_2} J_n(\beta_{j_1}) e^{i \Delta_{j_1 j_2} t + i n (\nu_{j_1} t + \phi_{j_1})} \sigma_{j_1}^+ \sigma_{j_2}^- + \text{h.c.}, \quad (3)$$

where $\Delta_{j_1 j_2} = \omega_{j_1} - \omega_{j_2}$, $\beta_j = \epsilon_j / \nu_j$, $J_n(\beta)$ is the n th Bessel function of the first kind. When we modulate the driving parameter $\nu_{j_1} = -\Delta_{j_1 j_2}$, and then neglecting the high-order oscillating terms, the Hamiltonian in the interaction picture can be approximated as

$$H_I(t) = g'_{j_1 j_2} \sigma_{j_1}^+ \sigma_{j_2}^- + \text{h.c.}, \quad (4)$$

where $g'_{j_1 j_2} = g_{j_1 j_2} J_1(\beta_{j_1}) e^{-i(\phi_{j_1} + \pi/2)}$. We can tune the coupling strength $g_{j_1 j_2}$ by changing β_{j_1} of the external modulation.

B. Conventional NHQC gate in DFS

The system configuration consists of three transmons, denoted as Q_1 , Q_a and Q_2 , as shown in figure 1 (a), they are arranged in a linear fashion, with qubit Q_a positioned in the middle. Neighboring transmon qubits are capacitively coupled, through appropriately biasing Q_1 and Q_2 as described in Section II A the Hamiltonian for this three-qubit system in the interaction picture can be approximated as

$$H(t) = g'_{1a} e^{-i\phi'_1} \sigma_1^+ \sigma_a^- + g'_{2a} e^{-i\phi'_2} \sigma_2^+ \sigma_a^- + \text{H.c.} \quad (5)$$

To illustrate the geometric nature of the time evolution operator, we introduce the following dressed states,

$$|b_1\rangle = |0\rangle_a \otimes \left[\sin\left(\frac{\theta}{2}\right) e^{-i\phi} |1\rangle_L + \cos\left(\frac{\theta}{2}\right) |0\rangle_L \right], \quad (6)$$

$$|b_2\rangle = |1\rangle_a \otimes \left[\cos\left(\frac{\theta}{2}\right) |1\rangle_L + \sin\left(\frac{\theta}{2}\right) e^{i\phi} |0\rangle_L \right], \quad (7)$$

where $|1\rangle_L = |01\rangle_{12}$, $|0\rangle_L = |10\rangle_{12}$, $\sin(\theta/2) = g'_{2a}/g$, $\cos(\theta/2) = g'_{1a}/g$, $g = \sqrt{g_{1a}^2 + g_{2a}^2}$, $\phi = \phi'_2 - \phi'_1$. Here, $\{|1\rangle_L, |0\rangle_L\}$ are computational basis of the logical qubit, and $S_C = \text{Span}\{|1\rangle_L, |0\rangle_L\}$ is the corresponding computational subspace. In terms of dressed states $|b_1\rangle$ and $|b_2\rangle$, the Hamiltonian (5) can be expressed as follows

$$H(t) = g(t) \left[e^{-i\phi'_1(t)} |b_1\rangle \langle a_1| + e^{i\phi'_1(t)} |b_2\rangle \langle a_2| + \text{H.c.} \right], \quad (8)$$

where $|a_1\rangle = |100\rangle_{a12}$, $|a_2\rangle = |011\rangle_{a12}$. To proceed, we decompose the Hamiltonian $H(t)$ into two parts, namely, $H(t) = H_1(t) + H_2(t)$, where $H_1(t) = g(t) e^{-i\phi'_1(t)} |b_1\rangle \langle a_1| + \text{h.c.}$ and $H_2(t) = g(t) e^{i\phi'_1(t)} |b_2\rangle \langle a_2| + \text{h.c.}$ It is evident that $|a_1\rangle$ and $|b_1\rangle$ belong to the single-excitation subspace $S_1 = \text{Span}\{|001\rangle, |010\rangle, |100\rangle\}$, while $|a_2\rangle$ and $|b_2\rangle$ belong to the two-excitation subspace $S_2 = \text{Span}\{|011\rangle, |101\rangle, |110\rangle\}$. Both S_1 and S_2 are DFSs since they are insensitive to collective dephasing. In simpler terms, Hamiltonian (8) can be seen as the sum of two independent Hamiltonians, each acting on a DFS. Consequently, collective dephasing does not influence any evolution starting from a state within these DFSs and governed by Hamiltonian (8). Given the independence between H_1 and H_2 , the temporal evolution operator takes the following form

$$U(t, 0) = U_1(t, 0) \otimes U_2(t, 0), \quad (9)$$

where $U_i(t, 0) = \mathcal{T} \exp\left(-i \int_0^t H_i(s) ds\right)$. For an orthonormal set of basis $\{|\psi_k(0)\rangle\}_{k=1}^3$ within the subspace S_i ($i \in \{1, 2\}$), through defining $|\psi_k(t)\rangle = U_i(t, 0) |\psi_k(0)\rangle$, we get another orthonormal basis set: $\{|\psi_k(t)\rangle\}_{k=1}^3$. Then the evolution operator $U_i(t, 0)$ can be expressed as

$$U_i(t, 0) = \sum_{k=1}^3 |\psi_k(t)\rangle \langle \psi_k(0)|. \quad (10)$$

To proceed, let's consider the third set of basis $\{|\mu_k(t)\rangle\}_{k=1}^3$, which span a space denoted as $M(t)$. When these ancillary basis vectors satisfy the boundary conditions:

$$|\mu_k(\tau)\rangle = |\mu_k(0)\rangle = |\psi_k(0)\rangle, \quad (11)$$

it follows that $M(\tau) = M(0)$, where τ is the total run time of the quantum gate. The continuous variation of $|\mu_k(t)\rangle$ causes $M(t)$ to move along a smooth and closed path \mathcal{C} in the N -dimensional space. The states $|\psi_k(t)\rangle$ can be expressed in terms of the ancillary basis as $|\psi_k(t)\rangle = \sum_l C_{lk}(t) |\mu_l(t)\rangle$, where $C_{lk}(t) = \langle \mu_l(t) | \psi_k(t) \rangle$. Boundary

conditions in Eq. (11) imply that $C_{lk}(0) = \delta_{lk} C_{ll}(0)$. The temporal evolution operator can then be written as $U(t, 0) = \sum_{l,k=1}^N C_{lk}(t) |\mu_l(t)\rangle \langle \mu_k(0)|$. Substituting this re-expressed $U(t, 0)$ into the Schrödinger equation, we obtain

$$\dot{C}_{lk}(t) = \sum_{m=1}^N i[A(t) - K(t)]_{lm} C_{mk}(t), \quad (12)$$

where $A_{lm}(t) = \langle \mu_l(t) | i\partial_t | \mu_m(t) \rangle$ and $K_{lm}(t) = \langle \mu_l(t) | H(t) | \mu_m(t) \rangle$. The formal solution of Eq. (12) is $C_{lk}(t) = \left[\mathcal{T} e^{i \int_0^t [A(s) - K(s)] ds} \right]_{lk}$.

For a conventional NHQC scheme [49], the Hamiltonian must be carefully designed so that there exists a set of basis vectors $\{|\mu_k(t)\rangle\}_{k=1}^N$ satisfying both Eq. (11) and the following condition

$$\langle \mu_l(t) | H(t) | \mu_m(t) \rangle = 0. \quad (13)$$

This equation implies $K = 0$, then we have

$$U(\tau, 0) = \sum_{l,k=1}^N \left[\mathcal{T} e^{i \int_0^\tau A(t) dt} \right]_{lk} |\mu_l(0)\rangle \langle \mu_k(0)|, \quad (14)$$

where $\mathcal{T} e^{i \int_0^\tau A(t) dt} = \mathcal{P} e^{i \oint_{\mathcal{C}} \mathcal{A}}$, with $\mathcal{A} = i \langle \mu_l(t) | d\mu_m(t) \rangle$, and \mathcal{P} is the path ordering along the closed path \mathcal{C} . The matrix $\mathcal{T} e^{i \int_0^\tau A(t) dt}$ depends only on the path \mathcal{C} , not on the detailed form of the system Hamiltonian, thus forming a non-Abelian geometric phase known as holonomy. We may write $U(\tau, 0) = U(\mathcal{C})$. To realize a universal quantum gate, at least two paths \mathcal{C}_1 and \mathcal{C}_2 are needed, such that $U(\mathcal{C}_1)$ and $U(\mathcal{C}_2)$ do not commute.

C. Single-qubit SR-NHQC gate in DFS

In the SR-NHQC scheme [37], the time evolution operator $U(t, 0)$ can be written in the following form

$$U(t, 0) = \sum_k e^{i\gamma_k(t)} |\mu_k(t)\rangle \langle \mu_k(0)|, \quad (15)$$

i.e. $|\psi_k(t)\rangle = e^{i\gamma_k(t)} |\mu_k(t)\rangle$. Inserting Eq. (15) into the Schrödinger equation, we have

$$\dot{\gamma}_k(t) = \langle \mu_k(t) | i\partial_t | \mu_k(t) \rangle - \langle \mu_k(t) | H(t) | \mu_k(t) \rangle, \quad (16)$$

when the parallel transport condition is satisfied, we get

$$\gamma_k(\tau) = \int_0^\tau dt \langle \mu_k(t) | i\partial_t | \mu_k(t) \rangle, \quad (17)$$

$\gamma_k(\tau)$ does not depend on the details of the system Hamiltonian and is of geometric origin.

To enable the implementation of universal single-logical-qubit gates in the DFS S_1 , the ancillary states are parametrized as follows:

$$\begin{aligned} |\mu_{d_1}\rangle &= |d_1\rangle, \\ |\mu_{b_1}(t)\rangle &= \cos\frac{\Omega(t)}{2} |b_1\rangle - i \sin\frac{\Omega(t)}{2} e^{i\phi'_1(t)} |a_1\rangle, \\ |\mu_{a_1}(t)\rangle &= -i \sin\frac{\Omega(t)}{2} e^{-i\phi'_1(t)} |b_1\rangle + \cos\frac{\Omega(t)}{2} |a_1\rangle. \end{aligned} \quad (18)$$

where $|d_1\rangle = |0\rangle_a \otimes [\cos(\frac{\theta}{2})|1\rangle_L - \sin(\frac{\theta}{2})e^{i\phi}|0\rangle_L]$ is a dark state for time evolution governed by H_1 and $\Omega(t) = \int_0^t g(s)ds$. It is noteworthy that $|\mu_{b_1}(0)\rangle = |b_1\rangle$, $|\mu_{a_1}(0)\rangle = |a_1\rangle$. Moreover, it can be verified that these ancillary states satisfy the parallel transport condition in Eq. (13). When $\Omega(\tau) = n \cdot 2\pi$, with n an integer, $|\mu_{b_1}(t)\rangle$ and $|\mu_{a_1}(t)\rangle$ are cyclic.

By using the boundary conditions, $U_1(\tau, 0)$ in the subspace $\text{span}\{|001\rangle, |010\rangle\}$ reads $U_1(\tau, 0) = e^{i\gamma_{b_1}(\tau)}|b_1(0)\rangle\langle b_1(0)| + |d_1\rangle\langle d_1|$. It can be rewritten as follows

$$U_1(\tau, 0) = |0\rangle_a\langle 0| \otimes e^{i\gamma_{b_1}/2} e^{-i\gamma_{b_1}\mathbf{n}_1 \cdot \boldsymbol{\sigma}/2}, \quad (19)$$

where $\mathbf{n} = (\sin(-\theta)\cos\phi, \sin(-\theta)\sin\phi, \cos(-\theta))^T$ is a unite vector in \mathbb{R}^3 and $\boldsymbol{\sigma} = (\sigma_x^{(L)}, \sigma_y^{(L)}, \sigma_z^{(L)})^T$ are the Pauli operators acting on S_C with explicit expressions as follows:

$$\begin{aligned} \sigma_x^{(L)} &= |1\rangle_L\langle 0| + |0\rangle_L\langle 1|, \\ \sigma_y^{(L)} &= -i|1\rangle_L\langle 0| + i|0\rangle_L\langle 1|, \\ \sigma_z^{(L)} &= |1\rangle_L\langle 1| - |0\rangle_L\langle 0|. \end{aligned} \quad (20)$$

Eq. (19) meaning that when the initial state of Q_a is $|0\rangle_a$, we can implement a universal single-qubit gate in the computational subspace S_C .

In a similar way, for $U_2(t, 0)$, the following ancillary states are considered

$$\begin{aligned} |\mu_{d_2}\rangle &= |d_2\rangle, \\ |\mu_{b_2}(t)\rangle &= \cos\frac{\Omega(t)}{2}|b_2\rangle - i\sin\frac{\Omega(t)}{2}e^{-i\phi_1'(t)}|a_2\rangle, \\ |\mu_{a_2}(t)\rangle &= -i\sin\frac{\Omega(t)}{2}e^{i\phi_1'(t)}|b_2\rangle + \cos\frac{\Omega(t)}{2}|a_2\rangle, \end{aligned} \quad (21)$$

where $|d_2\rangle = |1\rangle_a \otimes [\sin(\frac{\theta}{2})|1\rangle_L - \cos(\frac{\theta}{2})e^{i\phi}|0\rangle_L]$ is a dark state. These ancillary states satisfy the boundary and parallel transport conditions in Eq. (11) and Eq. (13). Then the temporal evolution operator in the subspace spanned by $\{|101\rangle, |110\rangle\}$ can be written as $U_2(t, 0) = \sum_{k=b_2, d_2} e^{i\gamma_k(t)}|\mu_k(t)\rangle\langle\mu_k(0)|$. By using Equations (21), it can be simplified into

$$U_2(\tau, 0) = |1\rangle_a\langle 1| \otimes e^{i\gamma_{b_2}(\tau)/2} e^{i\gamma_{b_2}\mathbf{n}_2 \cdot \boldsymbol{\sigma}/2}, \quad (22)$$

where $\mathbf{n}_2 = (\sin\theta\cos\phi, \sin\theta\sin\phi, \cos\theta)^T$ is also a unit vector in \mathbb{R}^3 , $\gamma_k(\tau)$ have the same form as Eq. (17) and therefore is a geometric phase. Equations (19) and (22) imply that, conditional on the initial state of the ancillary qubit Q_a , the temporal evolution operator $U(\tau, 0) = U_1(\tau, 0) \otimes U_2(\tau, 0)$ corresponds to the rotational gate with rotational axis \mathbf{n}_i and rotational angle γ_{bi} . Therefore, by choosing appropriate \mathbf{n}_i and γ_{bi} , it is possible to realize arbitrary single-qubit gates in the DFS S_C .

To ensure the robustness of SR-NHQC against the GCEs, we have found that in addition to the parallel transport and cyclic boundary conditions, there is a need for additional constraints to be imposed on the control [37]. These extra constraints are expressed as

$$\int_0^\tau \langle\psi_{ai}(t)|H_i(t)|\psi_{bi}(t)\rangle dt = 0, \quad (23)$$

with $i = 1$ and 2 . In the subsequent discussion, we set $i = 1$ and utilize the NOT gate as an illustrative example to demonstrate the implications of these conditions on the robustness of SR-NHQC gates. By substituting the expressions of $H_1(t)$, $|\psi_{b_1}(t)\rangle$ and $|\psi_{a_1}(t)\rangle$ into Eq.(23), we can rewrite the condition as $\int_0^\tau dt \exp[i(2\gamma_{b_1}(t) + \phi_1'(t))] = 0$. In accordance with the relationship $H_1(t) = \sum_{\alpha_1} i|\psi_{\alpha_1}(t)\rangle\langle\psi_{\alpha_1}(t)|$ and Eq. (8), we can deduce $\gamma_{b_1}(t) = \phi_1'(t)/\cos\Omega(t)$. Consequently, the aforementioned condition can be expressed in terms of $\phi_1'(t)$ and $\Omega(t)$ as:

$$\int_0^\tau dt e^{i \int_0^t [\phi_1'(t)/\cos\Omega(t)] dt} = 0. \quad (24)$$

It is noteworthy that the solution of Eq. (24) is not unique, and one possible solution is given by:

$$\phi_1'(t) = \begin{cases} 0 & 0 \leq t \leq \tau/4, \\ \gamma & \tau/4 < t \leq \tau/2, \\ 0 & \tau/2 < t \leq 3\tau/4, \\ \gamma & 3\tau/4 < t \leq \tau. \end{cases} \quad (25)$$

The shape of $\phi_1'(t)$ is shown in Fig. 2 (a). Furthermore, by letting $g = 2\pi/\tau$, we have $\Omega(\tau) = 2\pi$, the cyclic conditions of ancillary states in Eq. (18) and (21) are satisfied. To perform a NOT gate, the parameters need to be selected as follows: $\theta = \pi/2$, $\phi = 0$, and $\gamma = \pi$. When the initial state is $|0\rangle_L$, the temporal evolution of populations for $|0\rangle_L$ and $|1\rangle_L$ are presented in Fig. 2 (b).

In the presence of GCEs, the Hamiltonian can be expressed as

$$H'(t) = (1 + \delta)H(t), \quad (26)$$

where $H(t)$ represents the ideal Hamiltonian and δ signifies the strength of the error. Fig. 3 (a) depicts how the fidelity of the NOT gate changes with δ for three scenarios: the standard dynamical gate (DG), the conventional NHQC, and SR-NHQC. Compared to the DG and the conventional NHQC scenario, SR-NHQC exhibits superior robustness against GCEs, in the absence of decoherence.

Apart from control errors, decoherence poses another significant practical challenge in quantum computer development. Through the numerical simulation, we evaluate and compare the performance of various scenarios considering dephasing and relaxation effects. The following master equation is considered to describe the noisy temporal evolution of a transmon's density matrix $\rho(t)$

$$\dot{\rho}(t) = -i[H'(t), \rho(t)] + \mathcal{L}[\rho(t)], \quad (27)$$

where $H'(t)$ is the Hamiltonian given by Eq. (26), $\mathcal{L}[\rho(t)]$ is the Liouvillian given by the following equation

$$\mathcal{L}[\rho(t)] = \frac{\gamma_2^\varphi}{2} [2\Sigma_z \rho(t) \Sigma_z - \Sigma_z^2 \rho(t) - \rho(t) \Sigma_z^2], \quad (28)$$

where $\Sigma_z = \sum_j \sigma_j^z$ is the collective angular momentum of qubits involved in the gate operations, γ_2^φ is the pure collective dephasing rate.

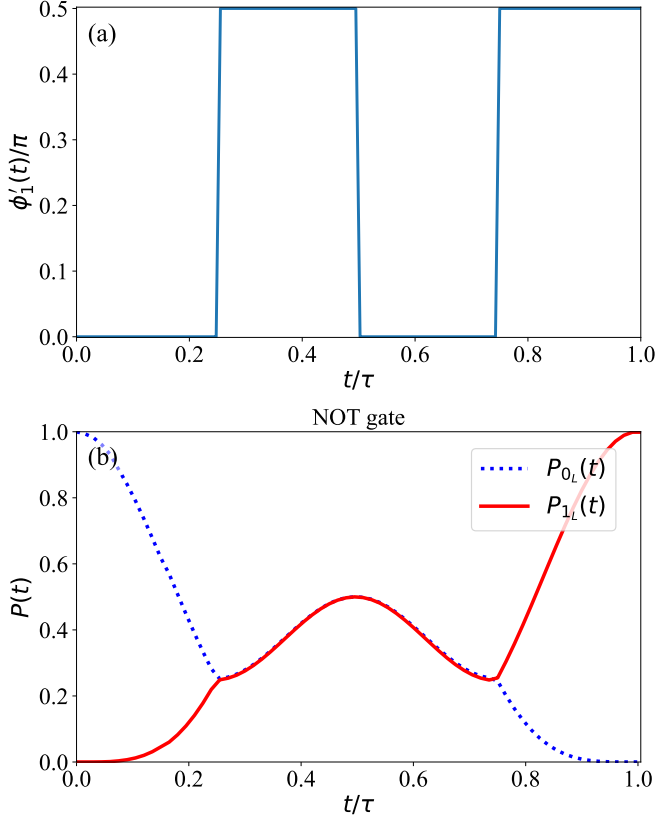


FIG. 2. (a) The shape of $\phi_1'(t)$ for the SR-NHQC NOT gate in DFS. (b) The temporal evolution of populations for states $|0\rangle_L$ (blue dotted line), and $|1\rangle_L$ (red solid line).

In the numerical simulation, we set the dephasing time $T_2 = 40\mu s$. These values are practical for transmon qubits [50]. The results are presented in Fig. 3 (b). Comparing it to Fig. 3 (a), it is evident that although the SR-NHQC scheme demonstrates remarkable robustness to GCE, decoherence considerably affects its performance. In contrast, the utilization of the decoherence-free subspace effectively mitigates the destructive effects of decoherence, demonstrated by higher gate fidelities of the SR-NHQC scheme in the DFS. We also present similar contents for the Hadamard gate in the Appendix A.

III. TWO-LOGICAL-QUBIT GATE

To achieve universal GQC in DFS, a nontrivial two-qubit gate is required besides single-qubit gates. This section introduces a proposal to perform an SR-NHQC CNOT gate in a DFS.

As illustrated in Fig. 1 (b), the setup comprises of four transmons, labeled as Q_j for $j \in \{1, 2, 3, 4\}$. When this configuration, Q_1 and Q_2 constitute a logical qubit L_1 , while Q_3 and Q_4 form another logical qubit L_2 . Notably, Q_2 is capacitively coupled to both Q_3 and Q_4 . The Hamiltonian that

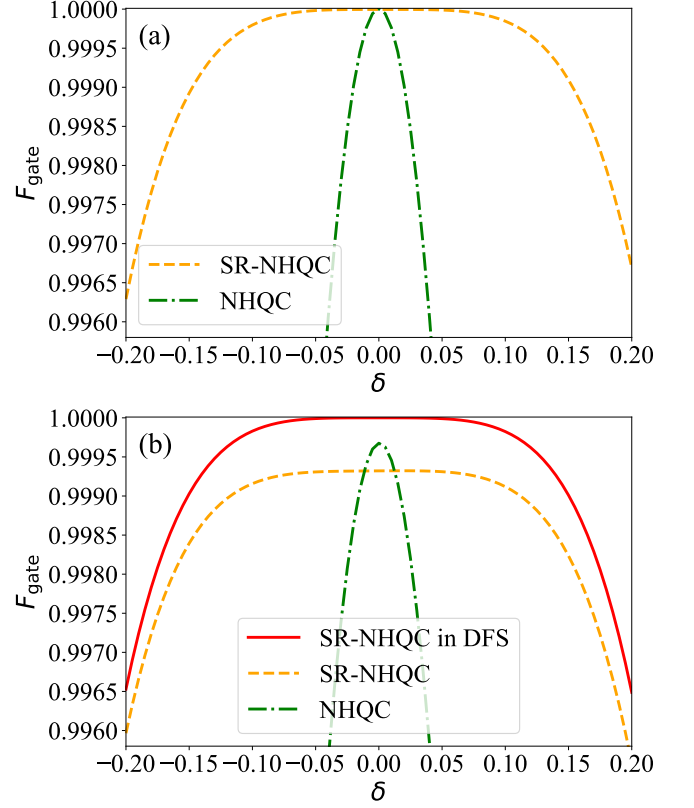


FIG. 3. (a) Gate fidelities of the NOT gate versus the amplitude of GCEs in the absence of decoherence. The results of three protocols are shown: SR-NHQC (orange solid line), conventional NHQC (green dashed line), and DG (red dot-dashed line). (b) Gate fidelities of the NOT gate in the presence of collective dephasing. We set $T_2 = 40\mu s$ in the simulation. Results of four protocols are shown: SR-NHQC in DFS (blue solid line), SR-NHQC (orange dotted line), NHQC (green dashed line), and DG (red dot-dashed line).

describes this system is expressed as follows

$$H(t) = \sum_{j=1}^4 H_{0,j} + H_{23} + H_{24}, \quad (29)$$

where $H_{0,j}(t) = \sum_{n=1,2} [n\omega_j - (n-1)\alpha] |n\rangle_j \langle n|$, and $H_{ij} = g_{ij} (\sigma_i^+ + \sigma_i^-) (\sigma_j^+ + \sigma_j^-)$. Here $|n\rangle_j$ represents the $(n+1)$ th energy level of Q_j , $\sigma_j^- = |0\rangle_j \langle 1| + \sqrt{2}|1\rangle_j \langle 2|$ is a ladder operator, α represents the transmon anharmonicity and g_{ij} maintains the same form as presented in Eq. (4). In contrast to gates involving a single logical qubit, the implementation of a two-logical-qubit gate necessitates the involvement of the second excited state $|2\rangle_j$. We then transform to a rotating frame defined by $H(t) \rightarrow U_0^\dagger(t)[H(t) - i\partial_t]U_0(t)$, where $U_0(t) = U_{0,3} \otimes U_{0,4} \otimes U_{0,2}$, and $U_{0,j} = \exp[-i \int_0^t dt' H_{0,j}(t')]$. For $j = 1, 3, 4$, we consider $\omega_j(t) = \omega_j + \epsilon_j \sin(\nu_j t + \phi_j)$, while $\omega_2(t) = \omega_2$ remains time independent. After disregarding high-order oscillating terms, the transformed Hamiltonian in

the two-excitation subspace can be expressed as

$$H = e^{-i\Phi_1(t)} \left(g'_{23} |11\rangle_{23} \langle 20| + g'_{24} |11\rangle_{24} \langle 20| \right) + \text{H.c.} \quad (30)$$

where $g'_{2j} e^{-i\Phi_1(t)} = g_{2j} \cdot \sqrt{2} J_1 \left(\frac{\epsilon_j}{\nu_j} \right) e^{-i(\phi_j + \pi/2)}$.

In deriving Eq. (30), we set $\nu_j = \Delta_{2j} - \alpha$, $\phi_3 = \varphi + \pi/2$, $\phi_4 = -\pi/2$. Eq. (30) can also be reformulated as

$$H = e^{-i\Phi_1(t)} \left(g'_{23} I_1 \otimes |1\rangle_2 \langle 2| \otimes |1\rangle_3 \langle 0| \otimes I_4 \right. \\ \left. + g'_{24} I_1 \otimes |1\rangle_2 \langle 2| \otimes I_3 \otimes |1\rangle_4 \langle 0| \right) + \text{H.c.}, \quad (31)$$

where $I_j = |0\rangle_j \langle 0| + |1\rangle_j \langle 1| + |2\rangle_j \langle 2|$ represents the identity operator of Q_j . Focusing on the two-excitation subspace, the effective Hamiltonian acting on this subspace can be written as

$$H_L(t) = G \left(e^{-i\Phi_1(t)} |B\rangle \langle A| + e^{i\Phi_1(t)} |A\rangle \langle B| \right), \quad (32)$$

where $|A\rangle \equiv |0200\rangle_{1234}$, $|B\rangle \equiv \sin(\theta/2)|10\rangle_L + \cos(\theta/2)|11\rangle_L$, with $|10\rangle_L = |0110\rangle_{1234}$, $|11\rangle_L = |0101\rangle_{1234}$, and $G = \sqrt{(g'_{23})^2 + (g'_{24})^2}$, $\theta = 2 \tan^{-1}(g'_{23}/g'_{24})$.

Similar to the single-logical-qubit case, a two-logical-qubit SR-NHQC gate, there exists a set of ancillary basis $\{|\nu_k(t)|k = A, B, D\}$ in the subspace spanned by $\{|A\rangle, |10\rangle_L, |11\rangle_L\}$. This basis states satisfy the following conditions

- 1) $|\nu_k(\tau)\rangle = |\nu_k(0)\rangle$, with τ the run time of the two-qubit gate,
- 2) $|\psi_k(t)\rangle = e^{i\gamma_k(t)} |\nu_k(t)\rangle$, where $\gamma_k(t)$ is a real function, $|\psi_k(t)\rangle \equiv U(t, 0) |\nu_k(0)\rangle$, with $U(t, 0)$ as the temporal evolution operator,
- 3) $\langle \nu_k(t) | H_L(t) | \nu_k(t) \rangle = 0$,
- 4) $\int_0^\tau dt \langle \psi_k | H_L(t) | \psi_l \rangle = 0$ for $k \neq l$.

Here $k, l = A, B, D$. By introducing a dark state defined as $|D\rangle = \cos(\theta/2)|10\rangle_L + \sin(\theta/2)e^{-i\varphi}|11\rangle_L$, the ancillary states can be parameterized as follows

$$|\nu_D(t)\rangle = |D\rangle, \\ |\nu_B(t)\rangle = \cos \frac{\Omega_T(t)}{2} |B\rangle - i \sin \frac{\Omega_T(t)}{2} e^{i\Phi_1(t)} |A\rangle, \quad (33) \\ |\nu_A(t)\rangle = -i \sin \frac{\Omega_T(t)}{2} e^{-i\Phi_1(t)} |B\rangle + \cos \frac{\Omega_T(t)}{2} |A\rangle,$$

where $\Omega_T(t) = \int_0^t G(s) ds$ and $\Omega_T(0) = 0$, leading to $|\nu_B(0)\rangle = |B\rangle$, $|\nu_A(0)\rangle = |A\rangle$. Condition 1) is satisfied when $\Omega(\tau)$ is an integer multiple of 2π . Together with Equation (32), condition (3) is automatically satisfied, while condition 4) can be rewritten as follows,

$$\int_0^\tau dt e^{i \int_0^t [\dot{\Phi}_1(t) / \cos \Omega(t)] dt} = 0. \quad (34)$$

In the following, we will demonstrate the implementation of a CNOT gate in the DFS $S_{2LQ} =$

$\text{span}\{|00\rangle_L, |01\rangle_L, |10\rangle_L, |11\rangle_L\}$, satisfying conditions 2) and 4), the subscript "2LQ" stands for "two-logical-qubit". First, we will describe how to perform a NOT gate in the subspace $S_{BD} \equiv \text{span}\{|B\rangle, |D\rangle\} = \text{span}\{|10\rangle_L, |11\rangle_L\}$. Utilizing conditions 1) and 2), the temporal evolution operator at time τ can be written as:

$$U(\tau, 0) = e^{i\gamma_A(\tau)} |A\rangle \langle A| + e^{i\gamma_B(\tau)} |B\rangle \langle B| + |D\rangle \langle D|, \quad (35)$$

where $\gamma_A(\tau) = -\gamma_B(\tau) = \int_0^\tau dt \langle \mu_A(t) | i \partial_t | \mu_A(t) \rangle$ represents a geometric phase. In the DFS S_{BD} , the temporal evolution operator can be expressed as:

$$U_L(\tau, 0) = e^{-i\gamma_g/2} e^{i\gamma_g \mathbf{n}_L \cdot \sigma_L / 2}, \quad (36)$$

where $\mathbf{n}_L = (\sin \theta \cos \varphi, \sin \theta \sin \varphi, -\cos \theta)$ is a unit vector in \mathbb{R}^3 , $\sigma_L = (\sigma_{XL}, \sigma_{YL}, \sigma_{ZL})^T$ with $\sigma_{XL} = |11\rangle_L \langle 10| + |10\rangle_L \langle 11|$, $\sigma_{YL} = -i|11\rangle_L \langle 10| + i|10\rangle_L \langle 11|$ and $\sigma_{ZL} = |11\rangle_L \langle 11| - |10\rangle_L \langle 10|$. This equation represents a rotation in the subspace S_{BD} around the axis \mathbf{n}_L by the angle γ_g .

To execute a NOT gate, we select $\theta = \pi/2$, $\varphi = 0$, $G = 2\pi/\tau$. The function $\Phi_1(t)$ is defined as follows to simultaneously satisfy conditions 2) and 4):

$$\Phi_1(t) = \begin{cases} 0 & 0 \leq t \leq \tau/4, \\ \pi & \tau/4 < t \leq \tau/2, \\ 0 & \tau/2 < t \leq 3\tau/4, \\ \pi & 3\tau/4 < t \leq \tau. \end{cases} \quad (37)$$

The resulting temporal evolution operator is $U_{BD} = |10\rangle \langle 11| + |11\rangle \langle 10|$. In the extended subspace spanned by $\{|00\rangle, |01\rangle, |10\rangle, |11\rangle\}$, the operator can be written as:

$$U_{2LQ} = |0\rangle_{1L} \langle 0| \otimes (|0\rangle_{2L} \langle 0| + |1\rangle_{2L} \langle 1|) \\ + |1\rangle_{1L} \langle 1| \otimes (|0\rangle_{2L} \langle 1| + |1\rangle_{2L} \langle 0|), \quad (38)$$

which precisely represents a CNOT gate.

To assess the robustness of the CNOT gate, we simulated its behavior under the influence of GCEs and collective dephasing, with the dynamics described by the master equation provided in Eqs. (27) and (28). The dephasing time was set to $T_2 = 40\mu\text{s}$. As illustrated in Fig. 4, the results indicate the superiority of SR-NHQC in suppressing GCEs in the presence of collective dephasing.

IV. CONCLUSION

In this paper, we introduced a novel approach to address the robustness issues of Nonadiabatic Holonomic Quantum Computation (NHQC) schemes, particularly focusing on the super-robust NHQC (SR-NHQC) framework, which significantly enhances the robustness against global control errors (GCEs). However, while SR-NHQC shows promise in mitigating GCEs, its prolonged operation time compared to conventional NHQC schemes renders it susceptible to decoherence effects, which are ubiquitous in various quantum computing platforms, thereby diminishing its practicality. To

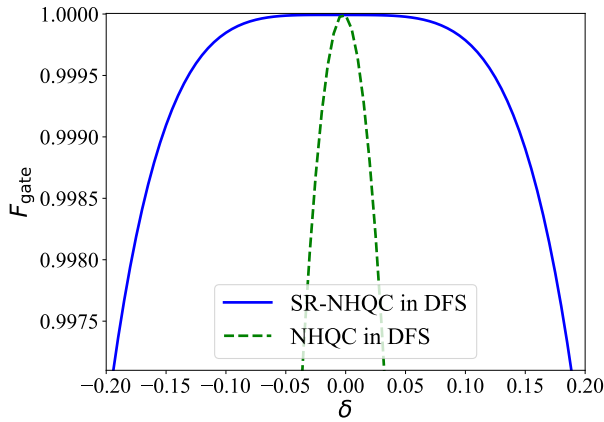


FIG. 4. Gate fidelities of the CNOT gate versus the amplitude of GCEs in the presence of decoherence. We set $T_2 = 40 \mu s$ in the simulation. The results of two protocols are shown: SR-NHQC in DFS (blue solid line) and the standard NHQC in DFS (green dashed line).

tackle this challenge, we proposed a solution termed SR-NHQC in Decoherence-Free Subspace (DFS) in this work. Our SR-NHQC in DFS approach leverages multiple transmon qubits coupled via capacitance to achieve universal single-qubit gates and a non-trivial two-qubit gate within DFSs. Moreover, the logical qubits in our scheme can be encoded in a scalable two-dimensional square lattice composed of superconducting qubits, a commonly adopted layout for superconducting quantum processors. To assess the practicality of SR-NHQC in DFS, we conducted numerical simulations evaluating various gate operations, including quantum NOT gates, Hadamard gates, and non-trivial two-qubit gates, under the presence of GCEs and collective dephasing. Comparative analysis confirms the superiority and practicality of our approach in alleviating GCEs compared to alternative schemes. Our proposed SR-NHQC in DFS scheme presents a promising avenue for enhancing the robustness of NHQC schemes while maintaining practicality in real-world quantum computing implementations. Future research can explore further optimizations and experimental validations to fully harness the potential of this approach in advancing quantum computing technologies.

ACKNOWLEDGMENTS

This research was partially supported by the Innovation Program for Quantum Science and Technology (Grant No. 2021ZD0302901) and National Natural Science Foundation of China (Grants No. 62002333 and No. 12135003).

Appendix A: Numerical results of the Hadamard gate

In this appendix, we demonstrate the implementation of an SR-NHQC Hadamard gate in a DFS and evaluate its perfor-

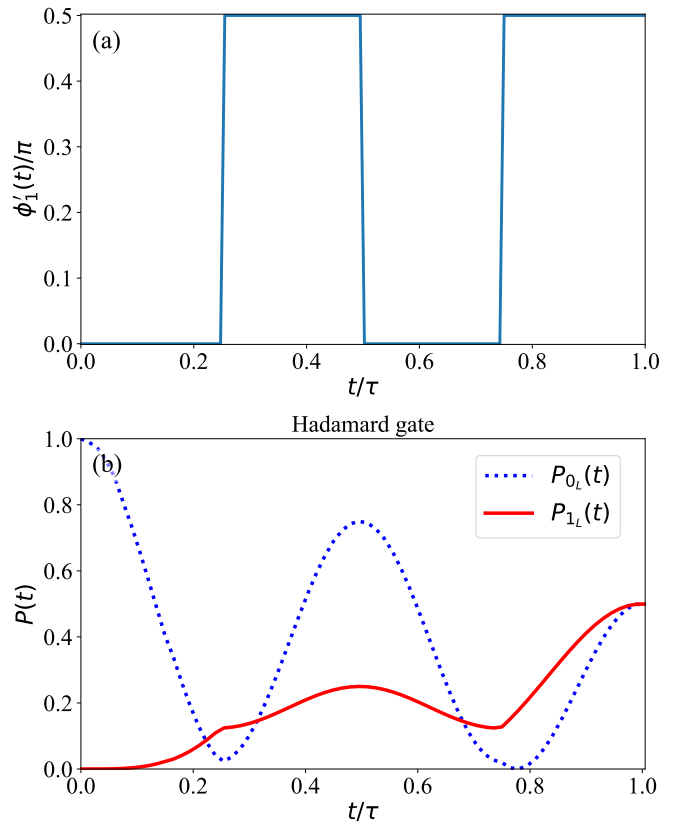


FIG. 5. (a) The shape of $\phi'_1(t)$ for the SR-NHQC Hadamard gate in DFS. (b) The temporal evolution of populations for $|0\rangle_L$ (blue dotted line), and $|1\rangle_L$ (red solid line).

mance in the presence of GCEs and decoherence.

To execute an SR-NHQC Hadamard gate in the DFS, one may set $\theta = \pi/4$, $\phi = 0$. The function $\phi'_1(t)$ retains the same form as given in Eq. (25) and its graph is shown in Fig. 5 (a). Starting from the initial state $|0\rangle_L$, the temporal evolution of the populations corresponding to $|0\rangle_L$ and $|1\rangle_L$ are depicted in Fig. 5 (b). In fig. 6 (a), we present how the fidelity of the Hadamard gate varies with the amplitude of GCEs, denoted as δ , for three scenarios: the standard dynamical gate (DG), the standard NHQC, and SR-NHQC. The results exhibit a pattern similar to that of the NOT gate, indicating that SR-NHQC offers enhanced robustness against GCEs in the absence of decoherence. Numerical evaluations of different scenarios' performance in the presence of collective are shown in Fig. 6 (b). The dephasing time T_2 in the numerical simulation matches that of the NOT gate described in the main text. It is evident that employing the decoherence-free subspace significantly mitigates the detrimental effects of collective dephasing, resulting in higher gate fidelities compared to the original SR-NHQC scheme.

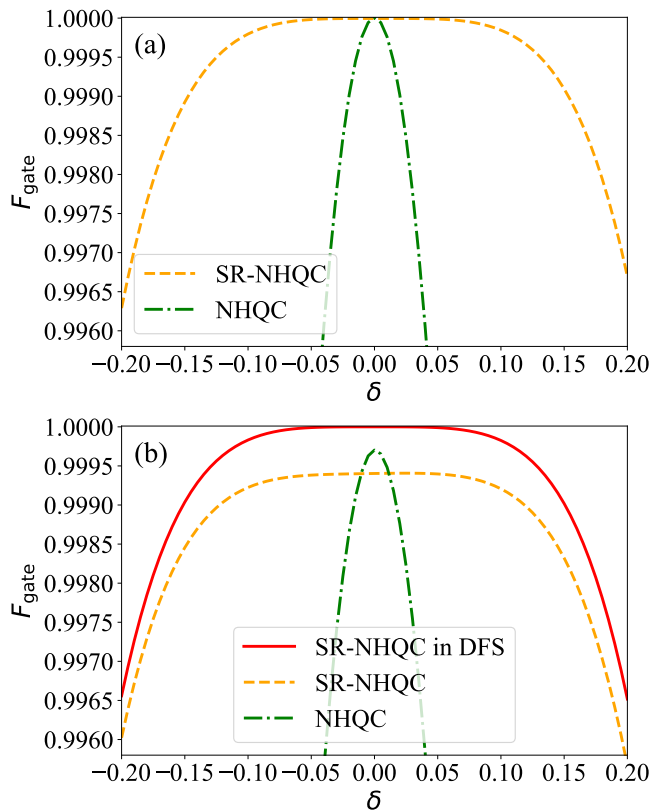


FIG. 6. (a) Gate fidelities of the Hadamard gate versus the amplitude of GCEs in the absence of decoherence. The results of three protocols are shown: SR-NHQC (orange solid line), conventional NHQC (green dashed line), and DG (red dot-ashed line). (b) Gate fidelities of the Hadamard gate in the presence of dephasing and relaxation. In the simulation, we set $T_2 = 40 \mu s$. Results of four protocols are shown: SR-NHQC in DFS (blue solid line), SR-NHQC (orange dotted line), NHQC (green dashed line), and DG (red dot-dashed line).

-
- [1] Michael A. Nielsen and Isaac L. Chuang, *Quantum computation and quantum information* (Cambridge University Press, 2000).
- [2] Ryszard Horodecki, Paweł Horodecki, Michał Horodecki, and Karol Horodecki, “Quantum entanglement,” *Reviews of Modern Physics* **81**, 865–942 (2009).
- [3] Zhaofeng Su, “Generating tripartite nonlocality from bipartite resources,” *Quantum Information Processing* **16**, 28 (2017).
- [4] Zhaofeng Su, Haisheng Tan, and Xiangyang Li, “Entanglement as upper bound for the nonlocality of a general two-qubit system,” *Physical Review A* **101**, 042112 (2018).
- [5] Carmen Palacios-Berraquero, Leonie Mueck, and Divya M. Persaud, “Instead of ‘supremacy’ use ‘quantum advantage’,” *Nature* **576**, 213 (2019).
- [6] Richard P Feynman, “Simulating physics with computers,” in *Feynman and computation* (cRc Press, 2018) pp. 133–153.
- [7] Zhaokai Li, Hui Zhou, Chenyong Ju, Hongwei Chen, Wenqiang Zheng, Dawei Lu, Xing Rong, Changkui Duan, Xinhua Peng, and Jiangfeng Du, “Experimental realization of a compressed quantum simulation of a 32-spin ising chain,” *Phys. Rev. Lett.* **112**, 220501 (2014).
- [8] Lieven M. K. Vandersypen, Matthias Steffen, Gregory Breyta, Costantino S. Yannoni, Mark H. Sherwood, and Isaac L. Chuang, “Experimental realization of shor’s quantum factoring algorithm using nuclear magnetic resonance,” *Nature* **414**, 883–887 (2001).
- [9] Nanyang Xu, Jing Zhu, Dawei Lu, Xianyi Zhou, Xinhua Peng, and Jiangfeng Du, “Quantum factorization of 143 on a dipolar-coupling nuclear magnetic resonance system,” *Phys. Rev. Lett.* **108**, 130501 (2012).
- [10] Enrique Martín-López, Anthony Laing, Thomas Lawson, Roberto Alvarez, Xiao-Qi Zhou, and Jeremy L. O’Brien, “Experimental realization of shor’s quantum factoring algorithm using qubit recycling,” *Nature Photonics* **6**, 773–776 (2012).
- [11] Lov K. Grover, “Quantum mechanics helps in searching for a needle in a haystack,” *Phys. Rev. Lett.* **79**, 325–328 (1997).
- [12] Patrick Rebentrost, Masoud Mohseni, and Seth Lloyd, “Quantum support vector machine for big data classification,” *Phys. Rev. Lett.* **113**, 130503 (2014).
- [13] Zhaokai Li, Xiaomei Liu, Nanyang Xu, and Jiangfeng Du, “Ex-

- perimental realization of a quantum support vector machine,” *Phys. Rev. Lett.* **114**, 140504 (2015).
- [14] Iris Cong, Soonwon Choi, and Mikhail D. Lukin, “Quantum convolutional neural networks,” *Nature Physics* **15**, 1273–1278 (2019).
- [15] Michael Brooks, “Beyond quantum supremacy: the hunt for useful quantum computers,” *Nature* **574**, 19–22 (2019).
- [16] Kaveh Khodjasteh and Lorenza Viola, “Dynamically error-corrected gates for universal quantum computation,” *Phys. Rev. Lett.* **102**, 080501 (2009).
- [17] Donovan Buterakos, Sankar Das Sarma, and Edwin Barnes, “Geometrical formalism for dynamically corrected gates in multiqubit systems,” *PRX Quantum* **2**, 010341 (2021).
- [18] Kenneth R. Brown, Aram W. Harrow, and Isaac L. Chuang, “Arbitrarily accurate composite pulse sequences,” *Phys. Rev. A* **70**, 052318 (2004).
- [19] Alexandre M. Souza, Gonzalo A. Álvarez, and Dieter Suter, “Robust dynamical decoupling for quantum computing and quantum memory,” *Phys. Rev. Lett.* **106**, 240501 (2011).
- [20] Jiang Zhang, Thi Ha Kyaw, Stefan Filipp, Leong-Chuan Kwek, Erik Sjöqvist, and Dianmin Tong, “Geometric and holonomic quantum computation,” *Physics Reports* **1027**, 1–53 (2023), geometric and holonomic quantum computation.
- [21] Yan Liang, Pu Shen, Tao Chen, and Zheng-Yuan Xue, “Nonadiabatic holonomic quantum computation and its optimal control,” *Science China Information Sciences* **66**, 180502 (2023).
- [22] Gabriele De Chiara and G. Massimo Palma, “Berry phase for a spin $1/2$ particle in a classical fluctuating field,” *Phys. Rev. Lett.* **91**, 090404 (2003).
- [23] Shi-Liang Zhu and Paolo Zanardi, “Geometric quantum gates that are robust against stochastic control errors,” *Phys. Rev. A* **72**, 020301 (2005).
- [24] P. J. Leek, J. M. Fink, A. Blais, R. Bianchetti, M. Göppl, J. M. Gambetta, D. I. Schuster, L. Frunzio, R. J. Schoelkopf, and A. Wallraff, “Observation of berry’s phase in a solid-state qubit,” *Science* **318**, 1889–1892 (2007).
- [25] S. Filipp, J. Klepp, Y. Hasegawa, C. Plonka-Spehr, U. Schmidt, P. Geltenbort, and H. Rauch, “Experimental demonstration of the stability of berry’s phase for a spin- $1/2$ particle,” *Phys. Rev. Lett.* **102**, 030404 (2009).
- [26] S. Berger, M. Pechal, A. A. Abdumalikov, C. Eichler, L. Steffen, A. Fedorov, A. Wallraff, and S. Filipp, “Exploring the effect of noise on the berry phase,” *Phys. Rev. A* **87**, 060303 (2013).
- [27] Paolo Zanardi and Mario Rasetti, “Holonomic quantum computation,” *Physics Letters A* **264**, 94–99 (1999).
- [28] L.-M. Duan, J. I. Cirac, and P. Zoller, “Geometric manipulation of trapped ions for quantum computation,” *Science* **292**, 1695–1697 (2001).
- [29] L.-A. Wu, P. Zanardi, and D. A. Lidar, “Holonomic quantum computation in decoherence-free subspaces,” *Phys. Rev. Lett.* **95**, 130501 (2005).
- [30] Zhang-qi Yin, Fu-li Li, and Peng Peng, “Implementation of holonomic quantum computation through engineering and manipulating the environment,” *Phys. Rev. A* **76**, 062311 (2007).
- [31] I. Kamleitner, P. Solinas, C. Müller, A. Shnirman, and M. Möttönen, “Geometric quantum gates with superconducting qubits,” *Phys. Rev. B* **83**, 214518 (2011).
- [32] Bao-Jie Liu, Xue-Ke Song, Zheng-Yuan Xue, Xin Wang, and Man-Hong Yung, “Plug-and-play approach to nonadiabatic geometric quantum gates,” *Phys. Rev. Lett.* **123**, 100501 (2019).
- [33] G. F. Xu, J. Zhang, D. M. Tong, Erik Sjöqvist, and L. C. Kwek, “Nonadiabatic holonomic quantum computation in decoherence-free subspaces,” *Phys. Rev. Lett.* **109**, 170501 (2012).
- [34] Zheng-Yuan Xue, Jian Zhou, and Z. D. Wang, “Universal holonomic quantum gates in decoherence-free subspace on superconducting circuits,” *Phys. Rev. A* **92**, 022320 (2015).
- [35] Zheng-Yuan Xue, Feng-Lei Gu, Zhuo-Ping Hong, Zi-He Yang, Dan-Wei Zhang, Yong Hu, and J. Q. You, “Nonadiabatic holonomic quantum computation with dressed-state qubits,” *Phys. Rev. Applied* **7**, 054022 (2017).
- [36] Nicklas Ramberg and Erik Sjöqvist, “Environment-assisted holonomic quantum maps,” *Phys. Rev. Lett.* **122**, 140501 (2019).
- [37] Bao-Jie Liu, Yuan-Sheng Wang, and Man-Hong Yung, “Superrobust nonadiabatic geometric quantum control,” *Phys. Rev. Res.* **3**, L032066 (2021).
- [38] A. A. Abdumalikov Jr, J. M. Fink, K. Juliusson, M. Pechal, S. Berger, A. Wallraff, and S. Filipp, “Experimental realization of non-Abelian non-adiabatic geometric gates,” *Nature* **496**, 482–485 (2013).
- [39] D.J. Egger, M. Ganzhorn, G. Salis, A. Fuhrer, P. Müller, P.Kl. Barkoutsos, N. Moll, I. Tavernelli, and S. Filipp, “Entanglement generation in superconducting qubits using holonomic operations,” *Phys. Rev. Applied* **11**, 014017 (2019).
- [40] Guanru Feng, Guofu Xu, and Guilu Long, “Experimental realization of nonadiabatic holonomic quantum computation,” *Phys. Rev. Lett.* **110**, 190501 (2013).
- [41] Hiromitsu Imai and Atsuo Morinaga, “Demonstration of pure geometric universal single-qubit operation on two-level atoms,” *Phys. Rev. A* **78**, 010302 (2008).
- [42] D. Leibfried, B. DeMarco, V. Meyer, D. Lucas, M. Barrett, J. Britton, W. M. Itano, B. Jelenković, C. Langer, T. Rosenband, and D. J. Wineland, “Experimental demonstration of a robust, high-fidelity geometric two ion-qubit phase gate,” *Nature* **422**, 412–415 (2003).
- [43] C. Zu, W.-B. Wang, L. He, W.-G. Zhang, C.-Y. Dai, F. Wang, and L.-M. Duan, “Experimental realization of universal geometric quantum gates with solid-state spins,” *Nature* **514**, 72–75 (2014).
- [44] Silvia Arroyo-Camejo, Andrii Lazariev, Stefan W. Hell, and Gopalakrishnan Balasubramanian, “Room temperature high-fidelity holonomic single-qubit gate on a solid-state spin,” *Nature Communications* **5**, 4870 (2014).
- [45] Yuhei Sekiguchi, Naeko Niikura, Ryota Kuroiwa, Hiroki Kano, and Hideo Kosaka, “Optical holonomic single quantum gates with a geometric spin under a zero field,” *Nature Photonics* **11**, 309–314 (2017).
- [46] X. Li, Y. Ma, J. Han, Tao Chen, Y. Xu, W. Cai, H. Wang, Y.P. Song, Zheng-Yuan Xue, Zhang-qi Yin, and Luyan Sun, “Perfect quantum state transfer in a superconducting qubit chain with parametrically tunable couplings,” *Phys. Rev. Applied* **10**, 054009 (2018).
- [47] S. A. Caldwell, N. Didier, C. A. Ryan, E. A. Sete, A. Hudson, P. Karalekas, R. Manenti, M. P. da Silva, R. Sinclair, E. Acala, N. Alidoust, J. Angeles, A. Bestwick, M. Block, B. Bloom, A. Bradley, C. Bui, L. Capelluto, R. Chilcott, J. Cordova, G. Crossman, M. Curtis, S. Deshpande, T. El Bouayadi, D. Girshovich, S. Hong, K. Kuang, M. Lenihan, T. Manning, A. Marchenkov, J. Marshall, R. Maydra, Y. Mohan, W. O’Brien, C. Osborn, J. Otterbach, A. Papageorge, J.-P. Paquette, M. Pelstring, A. Pollreno, G. Prawiroatmodjo, V. Rawat, M. Reagor, R. Renzas, N. Rubin, D. Russell, M. Rust, D. Scarabelli, M. Scheer, M. Selvanayagam, R. Smith, A. Staley, M. Suska, N. Tezak, D. C. Thompson, T.-W. To, M. Vahidpour, N. Vodrahalli, T. Whyland, K. Yadav, W. Zeng, and C. Rigetti, “Parametrically activated entangling gates using transmon qubits,”

Phys. Rev. Applied **10**, 034050 (2018).

- [48] Matthew Reagor, Christopher B. Osborn, Nikolas Tezak, Alexa Staley, Guenevere Prawiroatmodjo, Michael Scheer, Nasser Alidoust, Eyob A. Sete, Nicolas Didier, Marcus P. da Silva, Ezer Acala, Joel Angeles, Andrew Bestwick, Maxwell Block, Benjamin Bloom, Adam Bradley, Catvu Bui, Shane Caldwell, Lauren Capelluto, Rick Chilcott, Jeff Cordova, Genya Crossman, Michael Curtis, Saniya Deshpande, Tristan El Bouayadi, Daniel Girshovich, Sabrina Hong, Alex Hudson, Peter Karalekas, Kat Kuang, Michael Lenihan, Riccardo Manenti, Thomas Manning, Jayss Marshall, Yuvraj Mohan, William O'Brien, Johannes Otterbach, Alexander Papageorge, Jean-Philip Paquette, Michael Pelstring, Anthony Polloreno, Vijay Rawat, Colm A. Ryan, Russ Renzas, Nick Rubin, Damon Russel, Michael Rust, Diego Scarabelli, Michael Selvanayagam, Rodney Sinclair, Robert Smith, Mark Suska, Ting-Wai To, Mehrnoosh Vahidpour, Nagesh Vodrahalli, Tyler Whyland, Kamal Yadav, William Zeng, and Chad T. Rigetti, "Demonstration of universal parametric entangling gates on a multi-qubit lattice," *Science Advances* **4**, eaao3603 (2018), <https://www.science.org/doi/pdf/10.1126/sciadv.aao3603>.
- [49] Erik Sjöqvist, D. M. Tong, L. Mauritz Andersson, Björn Hessmo, Markus Johansson, and Kuldip Singh, "Non-adiabatic holonomic quantum computation," *New Journal of Physics* **14**, 103035 (2012).
- [50] Morten Kjaergaard, Mollie E. Schwartz, Jochen Braumüller, Philip Krantz, Joel I.-J. Wang, Simon Gustavsson, and William D. Oliver, "Superconducting qubits: Current state of play," *Annual Review of Condensed Matter Physics* **11**, 369–395 (2020).